


NAD⁺ supplementation prevents STING-induced senescence in CD8⁺ T cells by improving mitochondrial homeostasis

Bin Ye^{1,2,3,4}  | Yingting Pei^{1,2,3,4} | Lujing Wang^{1,2,3,4} | Dehao Meng^{1,2,3,4} |
 Yu Zhang^{1,2,3,4} | Shuang Zou^{1,2,3,4} | Henian Li^{1,2,3,4} | Jinying Liu⁵ |
 Ziyang Xie⁵ | Changhong Tian^{1,2,3,4} | Yuqi Jiang^{1,2,3,4} | Yu Qiao^{1,2,3,4} |
 Xu Gao^{1,2,3,4} | Yanfen Zhang⁵ | Ning Ma^{1,2,3,4}

¹Department of Biochemistry and Molecular Biology, Harbin Medical University, Harbin, China

²Key Laboratory of Cardiovascular Medicine Research (Harbin Medical University), Ministry of Education, Harbin, China

³Translational Medicine Center of Northern China, Harbin Medical University, Harbin, China

⁴Medical Science Institute of Heilongjiang Province, Harbin, China

⁵Department of laboratory diagnosis, Second Affiliated Hospital of Harbin Medical University, Harbin, China

Correspondence

Ning Ma

Email: maning2013@163.com

Yanfen Zhang

Email: zhangyanfen2005@163.com

Funding information

Reserve leader project of Heilongjiang Provincial leading talent Echelon, Grant/Award Number: 2018; Young Marshal Unveiling Project of Harbin Medical University, Grant/Award Number: HMUMIF-21025; Young & middle-aged Innovative Scientific Research Fund of the Second Affiliated Hospital of Harbin Medical University, Grant/Award Number: KYCX2019-14; Key projects of National Key Research and Development Program “Intergovernmental Cooperation in Science and Technology Innovation”, Grant/Award Number: 2022YFE0118200; Natural Science Foundation of Heilongjiang Province, Grant/Award Number: ZD2022H004

Abstract

Understanding the connection between senescence phenotypes and mitochondrial dysfunction is crucial in aging and premature aging diseases. Loss of mitochondrial function leads to a decline in T cell function, which plays a significant role in this process. However, more research is required to determine if improving mitochondrial homeostasis alleviates senescence phenotypes. Our research has shown an association between NAD⁺ and senescent T cells through the cGAS-STING pathway, which can lead to an inflammatory phenotype. Further research is needed to fully understand the role of NAD⁺ in T-cell aging and how it can be utilized to improve mitochondrial homeostasis and alleviate senescence phenotypes. We demonstrate here that mitochondrial dysfunction and cellular senescence with a senescence-associated secretory phenotype (SASP) occur in senescent T cells and tumor-bearing mice. Senescence is mediated by a stimulator of interferon genes (STING) and involves ectopic cytoplasmic DNA. We further show that boosting intracellular NAD⁺ levels with nicotinamide mononucleotide (NMN) prevents senescence and SASP by promoting mitophagy. NMN treatment also suppresses senescence and neuroinflammation and improves the survival cycle of mice. Encouraging mitophagy may be a useful strategy to prevent CD8⁺ T cells from senescence due to mitochondrial dysfunction. Additionally, supplementing with NMN to increase NAD⁺ levels could enhance survival

Bin Ye and Yingting Pei are contributed equally to this study.

rates in mice while also reducing senescence and inflammation, and enhancing mitophagy as a potential therapeutic intervention.

KEYWORDS

cGAS-STING, mitochondria, nicotinamide mononucleotide, SASP, senescence

1 | INTRODUCTION

Senescence refers to a decline in physiological functions that occurs with age. Cellular senescence is the gradual loss of intrinsic cell functions, such as communication and replication, which leads to the death or elimination of senescent cells by other cells, this process is necessary for life at the cellular level and reflects the aging of individual cells to a certain extent.^{1,2} As we age, there is an imbalance between pro-inflammatory and anti-inflammatory factors, resulting in a low-grade, chronic, and systemic inflammatory response known as inflammatory senescence.^{3,4} This state progressively increases and is closely related to immune senescence. Immunosenescence is a decrease in the precision and activity of the aging adaptive immune system due to thymic degeneration and other changes.⁵ This affects the development and function of T cells, B cells, NK cells, and monocytes.⁶ T cells are particularly important in immune response and disease resistance, and studies have found that they undergo the most significant changes during aging. The decline in T lymphocyte quantity and function is a major reason for the decline in immune responses during aging, making the relationship between T lymphocytes and aging an important focus of research on the immunological mechanism of aging.^{7,8}

In the age, memory T cells are extremely differentiated, leading to the loss of expression of costimulatory molecules such as CD27 and CD28, which leads to T cell senescence,^{9,10} and display the molecular hallmarks of aging (mitochondrial dysfunction and epigenetic remodeling).¹¹ In addition, T cell senescence can show signs of nuclear DNA damage, mitochondrial DNA (mtDNA) release, and telomere length shortening, and can activate aging-related signaling pathways.^{12–14} When DNA abnormally appears in the cytoplasm, the innate immune activation pathway of the cyclic guanosine monophosphate (GMP)-adenosine monophosphate (AMP) synthase (cGAS)-STING (stimulator of interferon genes) DNA-sensing pathway detects the presence of cytosolic is activated, which increases the release of interferon and triggers an inflammatory response to exclude foreign matters.¹⁵ Studies have reported cytoplasmic chromatin fragments in a variety of senescent primary cells and detected the activation of cGAS and STING proteins in

senescent cells triggered by various means.¹⁶ An important feature of senescent cells is senescence-related secretory phenotype (SASP). SASP can recruit immune cells, regulate their activities, and alter the tissue microenvironment.¹⁷ Some researchers believe that cells from patients with the age-related diseases ataxia and progeria exhibit extranuclear DNA aggregation that triggers an innate immune response via the DNA-sensitive cGAS-STING pathway.¹⁸ The cyclic GMP-AMP synthase (cGAS)-STING (stimulator of interferon genes) DNA-sensing pathway detects the presence of cytosolic DNA and triggers expression of inflammatory genes that lead to senescence or to the activation of defense mechanisms.^{19–22} In addition to enhancing inflammation, cGAS-STING activation also induces cell cycle arrest and accelerates cell senescence. This aging change is rapid, unlike the slower process by which telomere attrition brings the cell cycle to a standstill. In Alzheimer's disease mice, mitochondrial autophagy is weakened in the brain, and a large number of mtDNA is released into the cytoplasm, which activates the cGAS-STING pathway, inflammation and aging.^{23–25} These results suggest that the activation of STING signaling is also a potential target of immune cell senescence.

Mitochondrial dysfunction is one of the hallmarks of aging. The abnormal mitochondrial function leads to the decrease of mitochondrial membrane potential ($\Delta\Psi_m$), the increase of ROS level, the decrease of ATP synthesis.²⁶ Electron transport chain defects, and energy metabolism imbalance reduce the level of Nicotinamide adenine dinucleotide (NAD^+) in cells,²⁷ leading to irreversible cell growth arrest and cell senescence. NAD^+ is a key coenzyme in cellular energy metabolism and adaptive response to oxidative stress, and the NAD^+ -centered mammalian aging theory suggests that NAD^+ levels determine the rate and extent of aging.^{28,29} In recent years, studies have found that exogenous supplementation of NAD^+ precursor nicotinamide mononucleotide (NMN) can repair brain damage, improve brain mitochondrial respiratory function defects, and have a certain therapeutic effect on senile degenerative diseases which is an intermediate of the NAD^+ rescue synthesis pathway in mammals.³⁰ In the aged mouse model, NMN can improve the health status of aged mice by increasing NAD^+ levels. NMN treatment in

aged mice can inhibit the senescence of muscle stem cells, restore their function, and maintain the homeostasis regulation function of mitochondria.³¹ Long-term supplementation of NMN can reduce age-related weight gain, improve insulin sensitivity and eye function, increase bone mineral density, and enhance immunity.³² In addition, NMN supplementation can also improve the abnormalities of various metabolic indicators in aged mice, such as mitochondrial dysfunction and oxidative stress. Studies have reported that NMN's antiaging effect of the key is that it can improve or reverse age-related mitochondrial dysfunction.³³ However, little is known about the effect of NMN supplementation on T cell senescence progression.

In this study, we demonstrated that the development of T-cell senescence induced by malignant tumor cells is a general feature in the suppressive tumor microenvironment. We found that senescence causes an accumulation of cytoplasmic DNA, partly released from damaged mitochondria, triggering a STING-dependent senescence phenotype in the brain and in vitro. Boosting NAD⁺ levels with NMN removes damaged mitochondria by stimulating mitophagy and prevents senescence and SASP in aging models. Our findings link the tumor microenvironment directly to senescence, SASP, and impaired mitochondrial homeostasis.

2 | RESULTS

2.1 | Development of T cell senescence is a general feature of the tumor microenvironment

Tumor-reactive T cells are known to be suppressed and dysfunctional in the tumor microenvironment, which presents a major obstacle to successful tumor immunotherapy.^{34–36} We investigated the existence of senescent T cell populations in the tumor microenvironment in vivo. We used the murine mammary cancer cell line melanoma cell line B16F0 to establish melanoma tumors.³⁵ T cells from the spleen were isolated and analyzed after tumor diameters reached 10–15 mm. We observed elevated SA- β -gal⁺ CD8⁺ T cells from B16F10 tumor-bearing mice, but not in control tumor-free mice (Figure 1A,B). SASP-associated and senescent T cells were characterized by a decreased ratio of CD4⁺ and CD8⁺ T cells (Figure 1C). Compared with CD8⁺ T cells from tumor-free and B16F10-bearing mice, tumor-bearing mice displayed significantly higher expression (Figure 1D). Furthermore, CD8⁺ T cells from the spleen in B16F0-bearing mice displayed increased mRNA expression of genes encoding IL1- β , IL-6, TNF- α , and

IFN- γ relative to tumor-free mice (Figure 1E). We also evaluated the proteins level of senescence markers SASP by enzyme-linked immunosorbent assay (ELISA) (Figure 1F). Based on our findings, it appears that cancers may employ T cell senescence induction as a key tactic, potentially to cause T cell malfunction and avoid immune monitoring.

2.2 | Mitochondrial dysfunction in senescent CD8⁺ T cells

During the process of cellular aging, all functions can become damaged, including the important role of mitochondria as the energy factory of cells. As a result, we conducted an investigation into the effects of senescent CD8⁺ T cell dysfunction on mitochondrial function. Our findings align with recent studies that have reported the association between cellular senescence and mitochondrial defects.^{13,37,38} We found that senescent cells displayed higher reactive oxygen species (ROS) and lower ATP levels compared with control cells, while the mitochondrial membrane potential ($\Delta\Psi_m$) becomes depolarized (Figure 2A,B,C). As NAD⁺ plays important roles in DNA repair, mitochondrial homeostasis, senescence, and longevity in cells, worms, and mice. We examined here whether the NAD⁺ level and NAD⁺/NADH ratio were indeed disturbed in the senescent CD8⁺ T cells. As shown in our results, NAD⁺ levels and the NAD⁺/NADH ratio in senescent cells were both lower than those in the control cells (Figure 2D).

As the cytosolic mtDNA derived from damaged mitochondria is a potential inflammatory mediator, we sought to identify the mtDNA release in senescent CD8⁺ T cells. To quantify the mtDNA release amount, we separated cytosol from the whole cell for the qPCR experiment. Senescent T cells and healthy T cells were fractionated into cytoplasmic and nuclear fractions to quantify the level of DNA containing specific mitochondrial (mt-CytB, mt-16S, and mt-Dloop1) and nuclear (Tert) genes by qPCR, respectively.³⁹ Meanwhile, the cytoplasmic DNA extracted in this study was of high purity, and no obvious nucleolysis occurred. Consistently, the levels of free mtDNA in the cytoplasm of senescent CD8⁺ T cells were significantly higher than those of the control (Figure 2E), indicating that the release of mtDNA from damaged mitochondria into cytoplasm may serve as a possible trigger for inflammation and senescence in CD8⁺ T cells. Based on the findings, it can be concluded that T cell senescence leads to mitochondria damage resulting in increased ROS and membrane potential, decreased ATP levels, and ultimately the release of mtDNA into the cytoplasm.

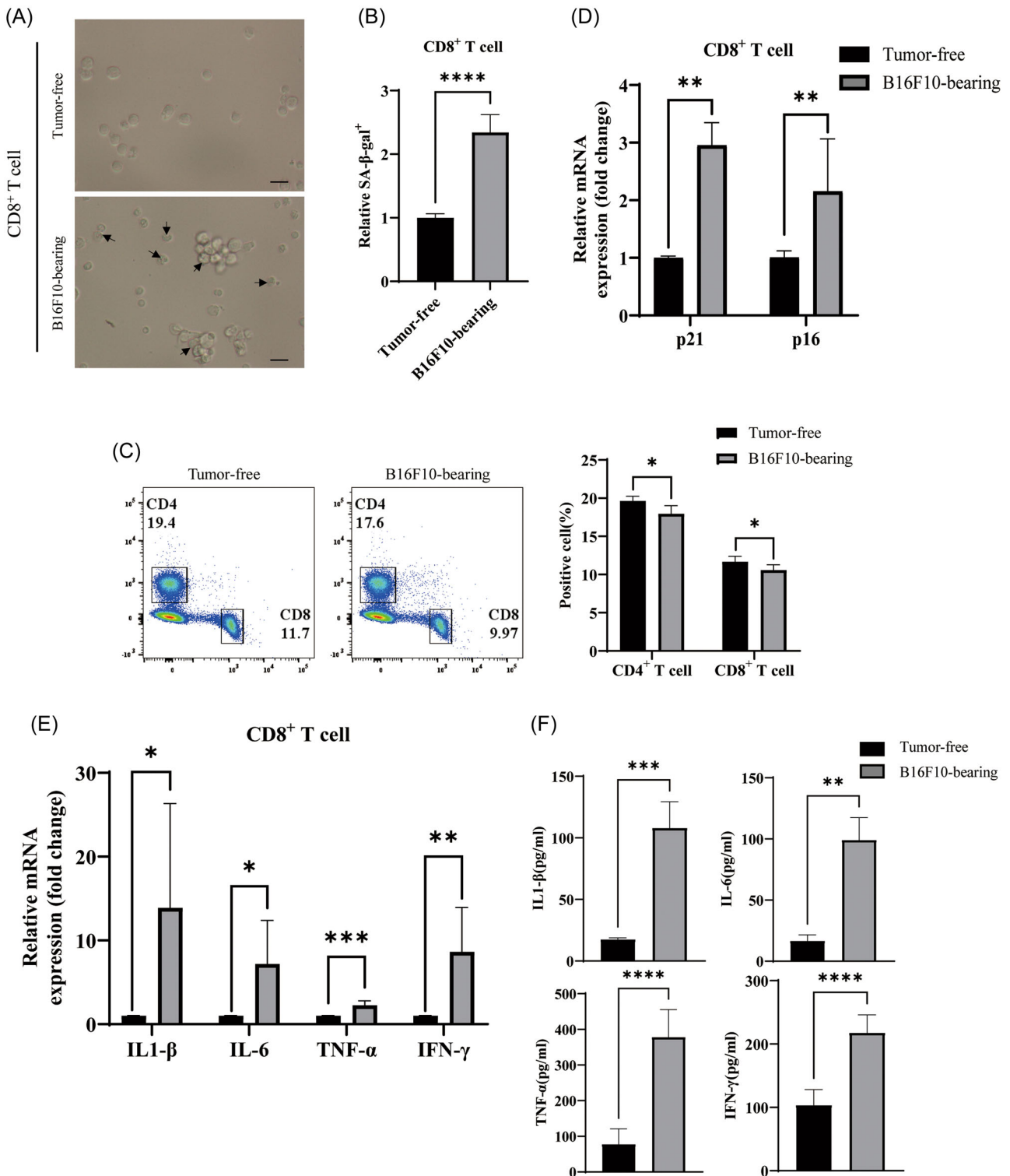


FIGURE 1 Development of T cell senescence is a general feature of the tumor microenvironment. Mice were subcutaneously injected with melanoma B16F10 cells to induce T cell senescence, and purified CD8⁺ T cells were sorted from the spleen, CD8⁺ T cells purified from spleen in tumor-free mice served as controls. (A) CD8⁺ T cells were incubated in the presence of plate-bound anti-CD3 (2 μg/mL) and anti-CD28 (1 μg/mL) for 3 days and then stained for SA-β-gal. Arrows indicate SA-β-gal⁺ T cells. Scale bars, 20 μm. (B) SA-β-gal activity was measured using the SPIDER-βGal Cellular Senescence Plate Assay Kit. Data are presented from three independent experiments. $n = 9$ different representative CD8⁺ T cells. (C) Lymphocytes were isolated from spleen and CD4⁺ T cell and CD8⁺ T cell were analyzed by flow cytometry, $n = 3$. (D, E) Relative genes expression for senescence (D), and SASP (E) between CD8⁺ T cells of tumor-free mice and B16F10-bearing mice. (F) The culture supernatants of activated CD8⁺ T cells from tumor-free mice and B16F10-bearing mice were prepared. The IL-1β, IL-6, TNF-α and IFN-γ level in the supernatants was detected by sandwich ELISA. All statistical significance was calculated by Student's *t* test. Data are shown as mean ± SD. * $p < 0.05$, ** $p < 0.01$, *** $p < 0.001$, **** $p < 0.0001$. SA-β-gal, senescence-associated β-galactosidase.

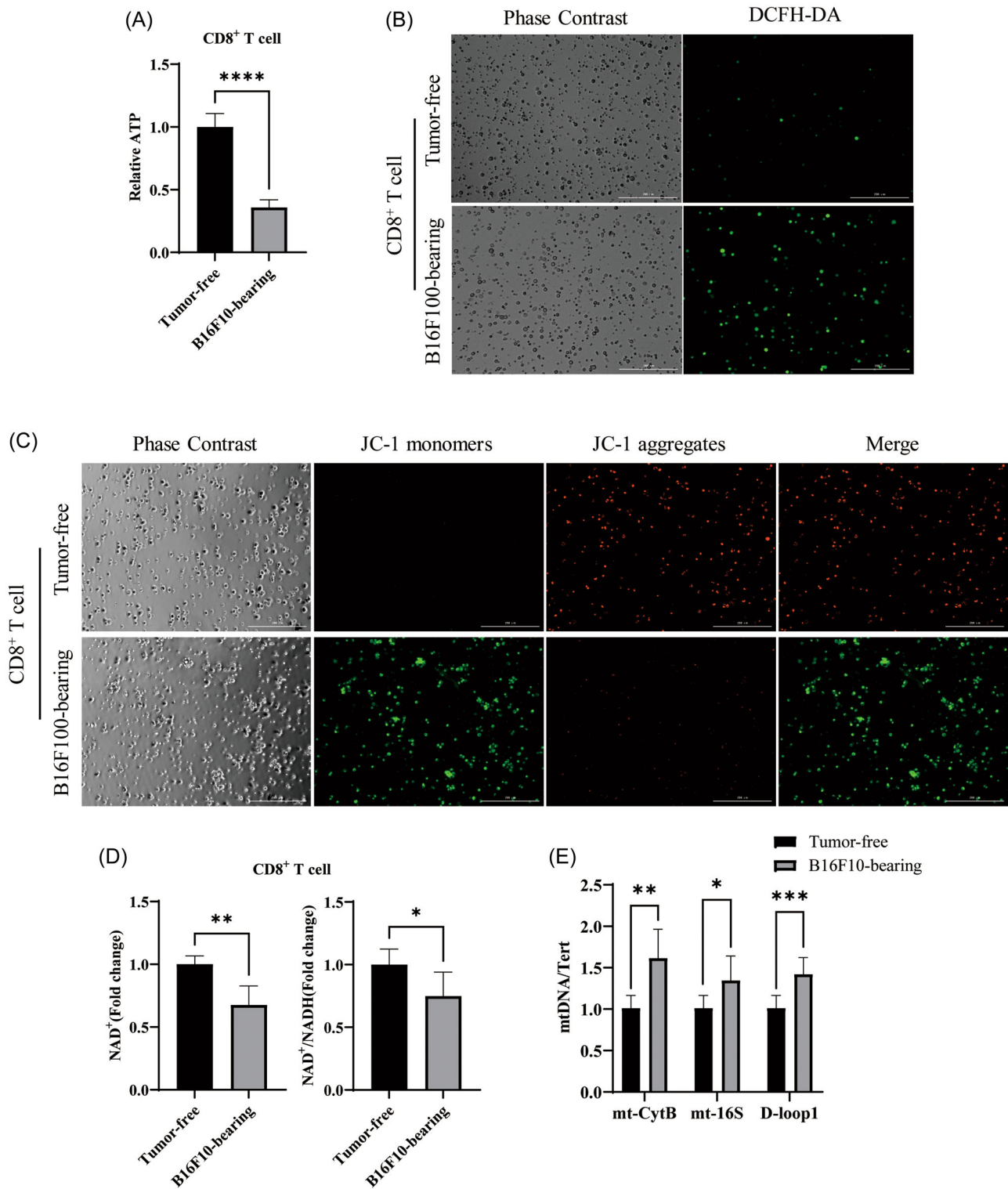


FIGURE 2 Mitochondrial dysfunction in senescent CD8⁺ T cells. (A) Cellular ATP level in senescent T cells (STs) and healthy T cells (HTs). (B) The representative ROS staining images in CD8⁺ T cells. Scar bar, 200 μ m. (C) Mitochondrial membrane potential ($\Delta\Psi$ m) was measured by Mitochondrial membrane potential assay kit with JC-1. Scar bar, 200 μ m. (D) The relative NAD⁺ level and NAD⁺/NADH ratio in STs and HTs. (E) qRT-PCR quantification of cytosolic DNA extracted from digitonin-permeabilized cytosolic extracts of control and senescent CD8⁺ T cells. Normalization was carried out as described in Methods. All statistical significance was calculated by Student's t-test. Data are shown as mean \pm SD. * p < 0.05, ** p < 0.01, *** p < 0.001, **** p < 0.0001. ROS, reactive oxygen species.

2.3 | The cGAS-STING-IRF3 pathway was activated in senescent CD8⁺ T cells

It has been previously reported that senescent cells release damaged DNA into the cytoplasm where it can activate the cytoplasmic DNA sensing STING-mediated pathway, which triggers the production of SASP factors, thereby promoting senescence phenotypes.^{20,21,39} We next tested whether the cGAS-STING pathway was activated in senescent CD8⁺ T cells. Likewise, the increased mRNA levels of cGAS, STING, TBK1, and IRF3 in senescent CD8⁺ T cells were confirmed by qRT-PCR, as well as the mentioned earlier IL-1 β , IL-6, TKF- α and IFN- γ (Figure 3A). Immunofluorescence also showed that the expression of STING was upregulated and clustered around the nucleus (Figure 3B). In addition to the activation of the cGAS and STING, the downstream targets, TBK1 and IRF3, were also activated in increased phosphorylated form, as well as the senescence-induced mRNA expression of several ISGs downstream of cGAS/STING: Ifit1, Isg15, and Ccl5 (Figure 3C). Expectedly, we found that the expression of cGAS and STING increased significantly in the senescent CD8⁺ T cell (Figure 3D). Unexpectedly, PINK1 was highly expressed which is a serine/threonine kinase, regulates mitochondrial dysfunction and initiates mitophagy.⁴⁰ However, the function of PINK1 in the aging process, especially in the CD8⁺ T cell, remains unknown.⁴¹ Taken together, these results suggested that the cGAS-STING-IRF3 pathway was activated in senescent CD8⁺ T cells.

2.4 | Inhibition of STING inhibits activation of the cGAS-STING and alleviates cellular senescence

Our research aimed to determine if the tumor micro-environment affects the aging of CD8⁺ T cells through the cGAS-STING pathway. To explore the effects of CD8⁺ T cell senescence, we used H-151 (2 μ M, MCE, #HY-12693), a specific inhibitor of STING. Our immunofluorescence results showed that STING enrichment was reduced in H-151-treated cells, and the treatment significantly reduced the expression of senescence signaling mediators (Figure 4A). Protein and mRNA level results revealed that the cGAS-STING pathway was activated during aging, but after using inhibitors, cGAS remained highly expressed (Figure 4B,D), while STING and its downstream molecules were significantly decreased (Figure 4B,C,D,E). Additionally, H-151 treatment resulted in a significant reduction in the expression of senescence signaling mediators and SASP, as

determined by ELISA and q-PCR (Figure 4F,G). We further investigated senescence in H-151 treated cells with an senescence-associated β -galactosidase (SA- β -gal) assay, which showed a decreased percentage of SA- β -gal-stained cells in H-151 treated cells compared to senescent CD8⁺ T cells (Figure 4H). This suggests that activated STING plays a key role in senescence phenotypes.

2.5 | NMN ameliorates STING-mediated senescence by improving mitochondrial functions and reduces cytoplasmic mtDNA

We then investigated whether boosting intracellular NAD⁺ levels with NMN could prevent senescence. The result shows that NMN (100 μ M, Absin, #abs47048054) supplementation for 3 days restored NAD⁺ levels and upregulated the NAD⁺/NADH ratio in senescent CD8⁺ T cells (Figure 5A). Consistent with the results observed in STs, there was a significant enrichment of mtDNA in the cytoplasmic fraction from senescent cells compared with control cells (Figure 5B). However, NMN supplementation reduced cytosolic mtDNA content (Figure 5B). Further, NMN decreased the ROS and mitochondrial membrane potential in CD8⁺ T cells, while the intracellular ATP was increased was observed after NMN treatment (Figure 5C–E).

Meanwhile, we have pretreated senescent CD8⁺ T cells with NMN and quantified the activation of the cGAS-STING pathway. The results showed that NMN could reduce the expression of cGAS, STING, p-TBK1 and p-IRF3, which was similar to that of STING inhibitor H-151 (Figure 5F,G,H,I). In addition, NMN supplementation could also significantly block the elevated secretion of IL-1 β , IL6, TNF- α and IFN- γ in the supernatant and reduce the mRNA of senescent CD8⁺ T cells (Figure 5J,K). Notably, the number of SA- β -gal positive cells was also significantly decreased after NMN treatment (Figure 5L). Taken together, these data directly indicated that NMN can significantly improve the senescence state of T cells and reduce the secretion of aging-related inflammatory factors via inhibition of the STING pathway.

2.6 | NMN prevents neuroinflammation and senescence in mice

Our studies suggest that preventing the generation of senescence in tumor-specific T cells is critical for antitumor immunity. Our current in vitro studies have indicated that activation of the cGAS-STING pathway is a checkpoint for control of T cell senescence and function

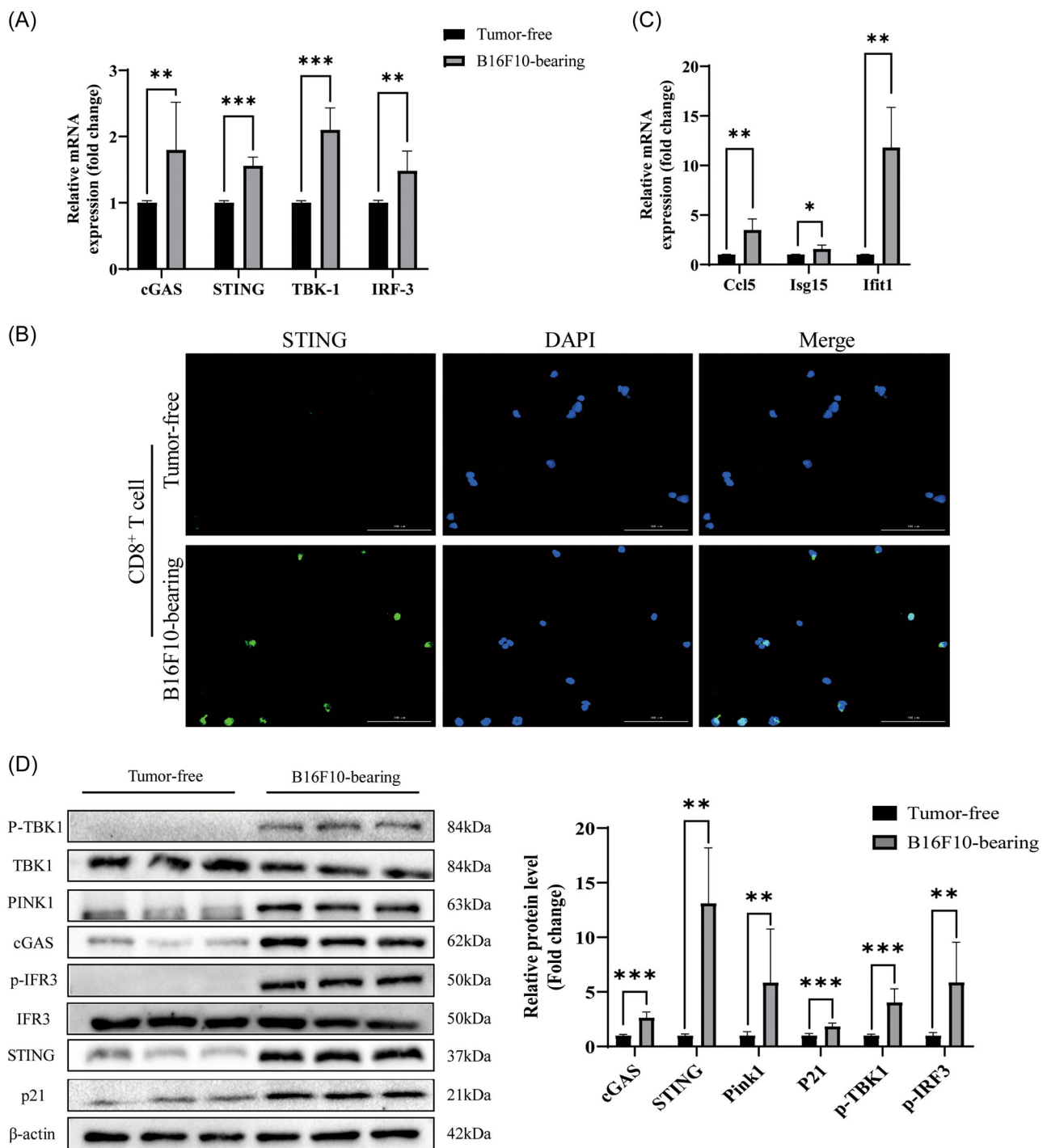


FIGURE 3 The cGAS-STING-IRF3 pathway was activated in senescent CD8⁺ T cells. (A) Expression of cGAS, STING, TBK-1, and IRF-3 in control HTs and STs analyzed by real-time qPCR. (B) Transcription levels of ISGs in CD8⁺ T cells from Tumor-free and B16F10-bearing mice were analyzed by qRT-PCR. (C) Immunofluorescence microscopic analysis of STING (green) in HTs and STs. Scar bar, 100 μm. DAPI was used to stain cell nuclei. (D) Protein concentrations of cGAS, STING, p-TBK1, TBK-1, p-IRF3, IRF-3, Pink1, and P21 were analyzed by Western blot analysis (left) and further quantitatively analyzed and compared against β-actin expression using densitometry (right). All statistical significance was calculated by Student's *t* test. Data are shown as mean ± SD. **p* < 0.05, ***p* < 0.01, ****p* < 0.001.

mediated by tumor cells. Therefore, we performed an intraperitoneal injection of NMN (500 mg/kg per mouse) once every 3 days in tumor-induced immunosenescence mice for 21 days. B16F10 tumor cells grew quickly in

untreated mice and NMN treatment promoted the inhibition of tumor growth. Furthermore, Kaplan–Meier survival analysis showed that mice treated with NMN survived longer than the other group (Figure 6A).

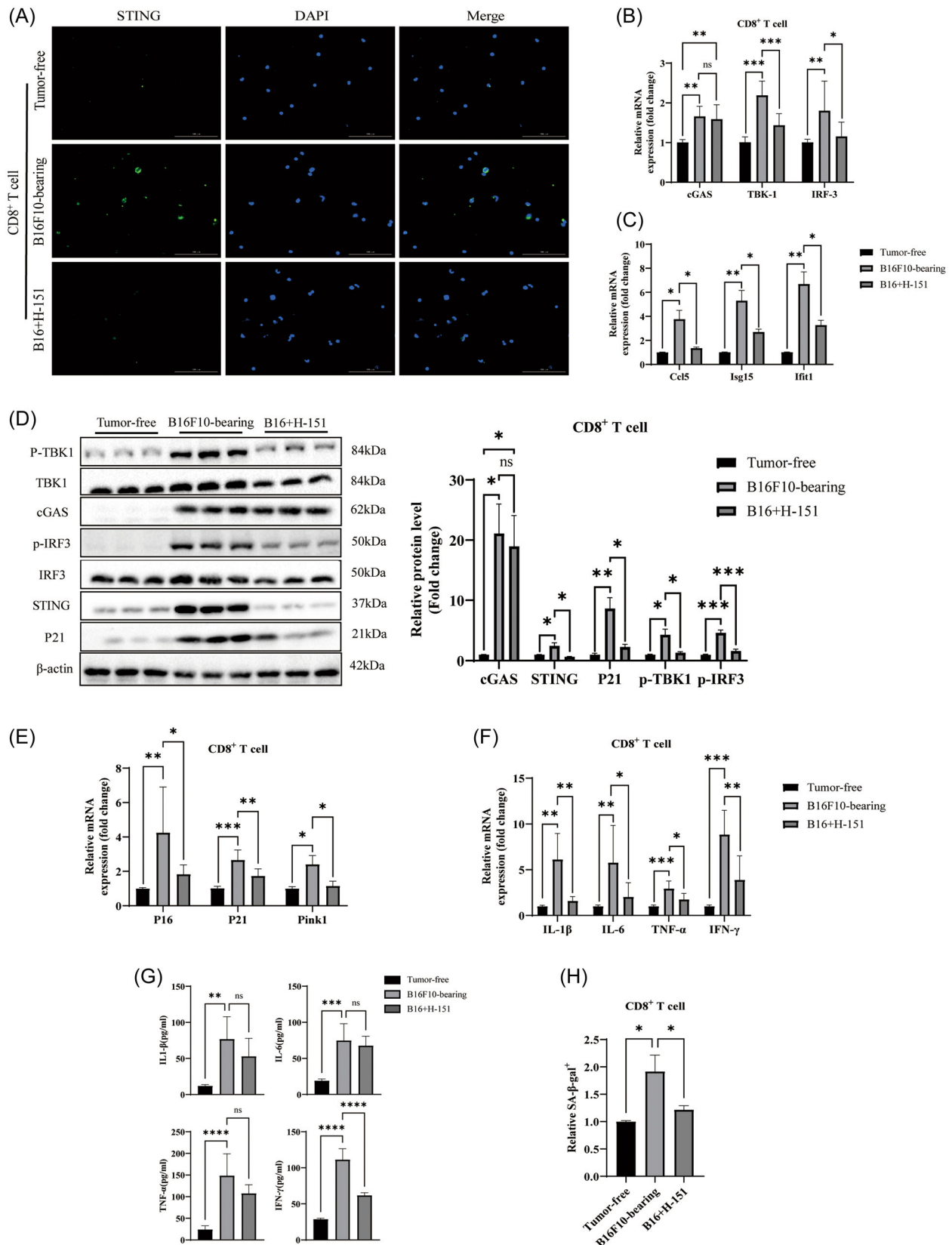


FIGURE 4 (See caption on next page).

We also compared the tumor formation rates of B16F10, and B16F10 + NMN in syngeneic C57BL/6 mice. As expected, tumor growth was significantly slowed in NMN treated mice (Figure 6B). In particular, we compared the spleens of three different groups of mice and found that the spleen tissue of tumor-induced senescence mice was significantly enlarged, which was alleviated by NMN treatment (Figure 6C). We then confirmed the molecular changes *in vivo* from different organs after NMN treatment. We observed that administration of NMN inhibited mRNA expression of IL-1 β , IL-6, IFN- γ , and P21 in the brain, liver, and spleen (Figure 6D,E,F). Furthermore, NMN treatment markedly increased CD4⁺ and CD8⁺ T cells fractions in spleen (Figure 6G). Meanwhile, the NAD⁺/NADH ratio of brain and spleen were also decreased in B16F10-treated mice and increased after NMN treatment (Figure 6H,I). In addition, NMN treatment markedly decreased cGAS, STING formation and prevented senescence in spleen (Figure 6J). According to the data, it appears that NMN treatment has the potential to improve antitumor activity, reduce neuroinflammation, improve aging conditions, and prolong the survival period of mice through the STING pathway. These findings are promising and may have significant implications for improving health outcomes.

3 | DISCUSSION

With the continuous extension of life expectancy, there is an urgent need to understand the common molecular pathways by which aging results in a progressively higher susceptibility to diseases. Our study suggests that disrupted mitochondrial balance is a significant factor in the aging of CD8⁺ T cells. We discovered that damaged mitochondria release cytoplasmic mtDNA, which partly activates STING and worsens senescence and SASP. Additionally, we found that raising NAD⁺ levels can enhance mitochondrial function, decrease cytoplasmic

DNA, and prevent STING activation, which ultimately improves motor function, prevents inflammation, and slows the aging process in CD8⁺ T cells.

Mitochondrial dysfunction is closely linked with senescence phenotypes, and compromised mitophagy is considered a hallmark of neurodegenerative diseases.^{42,43} Inflammatory cytokines play a crucial role in initiating and sustaining cellular senescence, thereby triggering an innate immune response that removes senescent cells. Inflammation and autoimmune syndromes are frequently observed in aging individuals.^{44–46} Cellular senescence is widely believed to be a major mechanism of aging-related dysfunction, resulting from irreversible growth arrest induced by telomere shortening or various stress responses, including DNA damage.⁴⁴ To prevent chromosomal instability and safeguard genomic stability, DNA damage responses activate permanent cell cycle arrest. T cells can undergo senescence due to both short-term and long-term stressors. Naive T cells usually undergo telomere shortening due to homeostatic proliferation, while memory T cells have shorter telomeres due to their increased replicative history. Additionally, the DNA damage response is activated in T cells proliferating in response to antigen recognition, which may result in less effective vaccine responses in older individuals.^{47,48} These findings underscore the critical role of inflammatory responses in aging, potentially linked to the upregulation of the STING pathway. Here, we observed accumulation of cytoplasmic dsDNA *in vitro*, which stimulates the STING pathway. Activation of STING subsequently initiates a robust proinflammatory response and senescence, associated with the deficient health span in our model mice. Senescence phenotypes are rescued by inhibiting of STING, suggesting that STING is a central regulator of this phenotype.

As we age, there is a reduction in the NAD⁺ pool experienced by cells and tissues. This can lead to a loss of mitochondrial homeostasis and senescence phenotypes in senescent CD8⁺ T cells.^{49,50} Damaged mitochondria can also activate inflammatory mediators, contributing to senescence phenotypes. To inhibit senescence and SASP in senescent cells, it is important to explore ways to improve

FIGURE 4 Inhibition of STING inhibits activation of the cGAS-STING and alleviates cellular senescence. (A) Immunofluorescence microscopic analysis of STING (green) in HTs, STs, and treated with H-151. Scale bars, 100 μ m. DAPI was used to stain cell nuclei. (B) Expression of cGAS, TBK-1, and IRF-3 in control HTs, STs, and treated with H-151 analyzed by real-time qPCR. (C) Transcription levels of ISGs in HTs, STs and treated with H-151 were analyzed by qRT-PCR. (D) Protein concentrations of cGAS, STING, p-TBK1, TBK-1, p-IRF3, IRF-3, Pink1, and P21 were analyzed by Western blot analysis (left) and further quantitatively analyzed and compared against β -actin expression using densitometry (right). (E, F) qPCR analysis for senescence markers P16 and P21 (E) and SASP in HTs, STs and treated with H-151 (F). (G) The culture supernatants of activated HTs, STs and treated with H-151 were prepared. The IL-1 β , IL-6, TNF- α and IFN- γ level in the supernatants was detected by sandwich ELISA. (H) SA- β -gal activity was measured using the SPiDER- β Gal Cellular Senescence Plate Assay Kit. Data are presented from three independent experiments. Data shown are means \pm SD from three independent experiments. * p < 0.05, ** p < 0.01, *** p < 0.001. One-way ANOVA was performed. ANOVA, analysis of the variance; SA- β -gal, senescence-associated β -galactosidase.

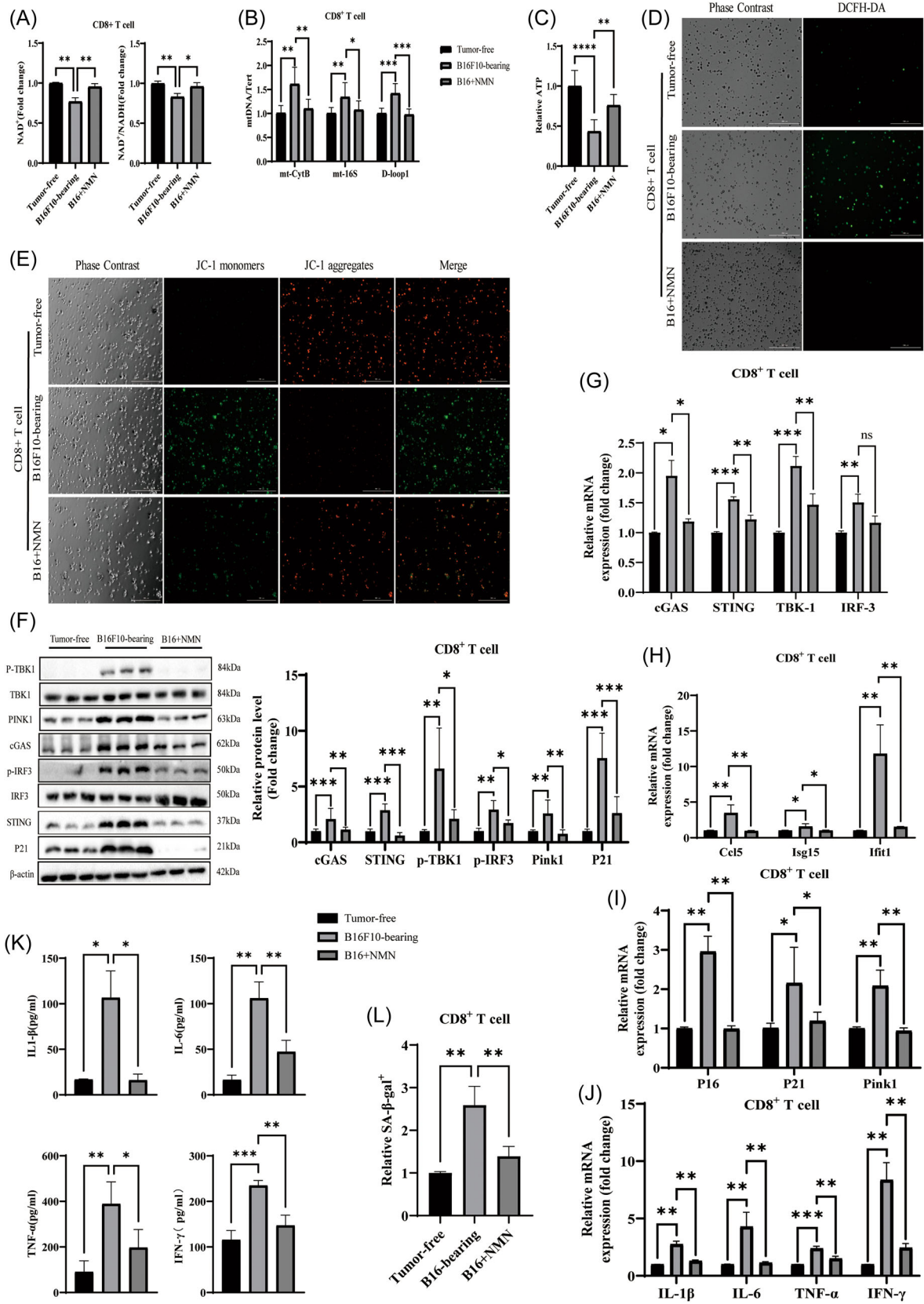


FIGURE 5 (See caption on next page).

mitochondrial function.^{51,52} Studies have shown that mitochondrial stress can increase levels of proinflammatory cytokines and senescence. In CD8⁺ T cells of tumor-bearing mice, impaired mitochondria can lead to the release of mtDNA into the cytoplasm, which activates senescence phenotypes. Boosting cellular concentration of NAD⁺ can help suppress the accumulation of cytoplasmic dsDNA by activating mitophagy, which clears damaged mitochondria. These findings suggest that enhancing mitophagy through NMN can prevent senescence in tumor-bearing models.

Boosting cellular concentration of NAD⁺ can suppress the accumulation of cytoplasmic dsDNA by activating mitophagy, which clears damaged mitochondria.⁵³ These findings suggest that enhancing mitophagy through NMN can prevent senescence in tumor-bearing models. Additionally, studies have reported that NMN treatment can downregulate the activation of cGAS-STING pathway in senescent mouse brains, reducing neuroinflammation.⁵³ NMN can also improve nonhomologous end joining-mediated double-strand break repair by increasing NAD⁺/SIRT1 signaling.⁵⁴ Other NAD⁺-dependent sirtuin members, including SIRT6 and SIRT3, also contribute to the DNA repair improvements by NAD⁺ supplementation. It is noteworthy that in addition to the regulation of senescence by mitophagy, NMN may also bring health benefits to tumor-bearing mice through multiple other mechanisms.

We discovered that NMN treatment had varying effects on protein levels in spleen of senescent mice. NMN reduced the levels of cGAS and STING proteins, while it increased those protein levels in the spleen of senescent mice. This difference may be due to varying NAD⁺ levels in young and senescent mice, as well as age or localized drug effects on specific tissues. It's common knowledge that NAD⁺ levels decrease with age. In our experiment, we used tumor-bearing mice and treated them with NMN, resulting in stable weight gain, slower tumor progression, and longer survival periods compared to the untreated group. However, further NAD⁺ supplementation may disturb the NAD⁺ metabolome

balance and have unintended effects. Additionally, we only checked the brain and spleen in our experiment, so we're unsure if NMN supplementation would have similar effects in other tissues. For senescent mice, our data and previous reports showed a significant decrease in NAD⁺ levels compared to young mice. As NAD⁺ is crucial for various molecular processes, including DNA repair, mitochondrial functions, and cellular senescence, NAD⁺ supplementation is critical and beneficial in settings where NAD⁺ levels are low, such as tumor-bearing or normal aging. However, it remains to be determined if NAD⁺ supplementation is advisable for healthy young humans.

In conclusion, our results demonstrate a correlation between the cGAS-STING pathway and inflammatory and senescence phenotypes. We found that the activation of cGAS-STING is partly caused by cytoplasmic dsDNA released from damaged mitochondria, which occurs in tumor-induced senescence of CD8⁺ T cells. Furthermore, we observed that supplementing with NAD⁺ can help remove damaged mitochondria through mitophagy, which inhibits inflammation and senescence in senescent models. Therefore, our data suggest that targeting the maintenance of mitochondrial quality could have potential roles in preventing senescence and inflammation in age-related diseases.

4 | MATERIALS AND METHODS

4.1 | Animals

C57BL/6 (B6) mice were primarily used in this study. Animals were maintained on a 12-h light/12-h dark cycle at 22°C, and Standard Laboratory Diet and water were given ad libitum. Mice were randomly assigned to control or experimental groups. All animal experimental protocols were approved by Ethics Committee of Harbin Medical University and conformed to the Guide for the Care and Use

FIGURE 5 NMN ameliorates STING-mediated senescence by improving mitochondrial functions and reduces cytoplasmic mtDNA. (A) The relative NAD⁺ level and NAD⁺/NADH ratio in HTs, STs and treated with NMN. (B) DNA was harvested from cytoplasmic and nuclear fractions of HTs, STs with or without NMN treatment, and mtDNA/Tert was analyzed by qPCR. *n* = 4 cultures per group. (C) Cellular ATP level in HTs, STs with or without NMN treatment. (D) The representative ROS staining images in CD8⁺ T cells. Scar bar, 200 μm. (E) Mitochondrial membrane potential was measured by Mitochondrial membrane potential assay kit with JC-1 respectively. Scar bar, 200 μm. (F) Senescence and SASP markers were analyzed by immunoblotting in CD8⁺ T cells, including cGAS, STING, p-TBK1, p-IRF3, Pink1 and P21 protein levels. Quantification of protein levels are shown in the right. (G) Expression of cGAS, STING, TBK-1, and IRF-3 in control HTs, STs with or without NMN treatment analyzed by real-time qPCR. (H) Transcription levels of ISGs in HTs, STs with or without NMN treatment were analyzed by qPCR. (I) Expression of senescence markers P16 and p21 in control HTs, STs with or without NMN treatment analyzed by real-time qPCR. (J, K) The culture supernatants and mRNA of activated HTs, STs with or without NMN treatment were prepared. The IL-1β, IL-6, TNF-α and IFN-γ level in the supernatants was detected by sandwich ELISA (K) and relative genes expression were analyzed by qRT-PCR (J). (L) SA-β-gal activity was measured of CD8⁺ T cell using the SPiDER-βGal Cellular Senescence Plate Assay Kit. Data shown are means ± SD from three independent experiments. **p* < 0.05, ***p* < 0.01, ****p* < 0.001. One-way ANOVA was performed. ANOVA, analysis of the variance; ROS, reactive oxygen species; SA-β-gal, senescence-associated β-galactosidase.

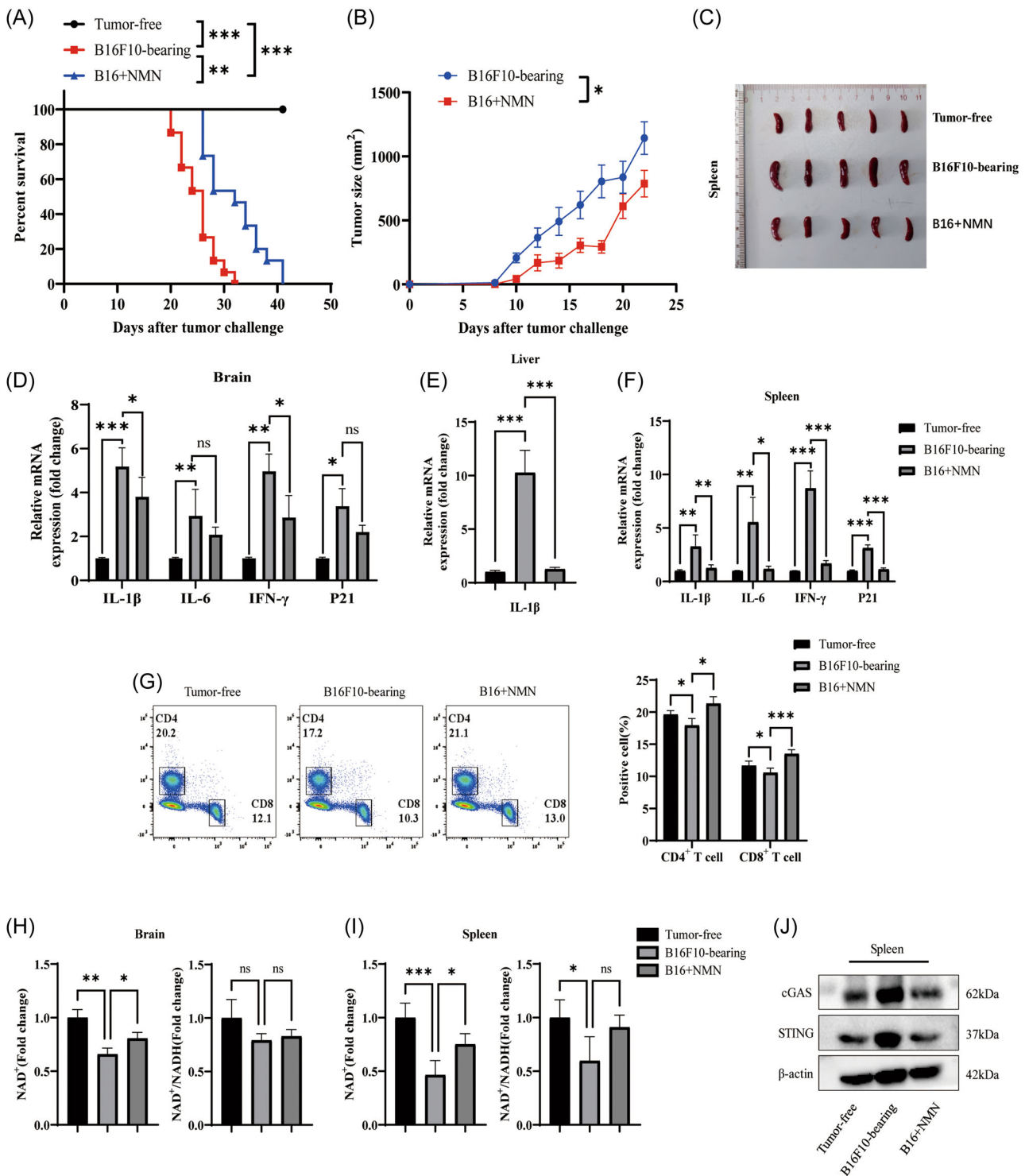


FIGURE 6 NMN prevents neuroinflammation and senescence in mice. (A, B) Tumor volume and Kaplan-Meier survival curves for C57BL/6 mice inoculated with PBS, B16F10 cells, and B16F10 cells+NMN. (C) Photograph of spleen from mice that were challenged by PBS, B16F10 cells, and B16F10 cells + NMN ($n = 5$). (D, E, F) Relative mRNA levels of IL-1 β , IL-6, IFN- γ , and P21 in the brain, liver, and spleen were analyzed by real-time qPCR. (G) Lymphocytes were isolated from spleen and CD4⁺ T cell and CD8⁺ T cell were analyzed by flow cytometry, $n = 3$. (H) The relative NAD⁺ level and NAD⁺/NADH ratio in Brain, Liver and Spleen. (I) Protein concentrations of cGAS, and STING were analyzed by Western blot analysis. Data shown are means \pm SD from three independent experiments. * $p < 0.05$, ** $p < 0.01$, *** $p < 0.001$. Log-rank test (A) or one-way ANOVA (D-H) were performed. ANOVA, analysis of the variance.

of Laboratory Animals published by the US National Institutes of Health.

To analyze T cell responses in the tumor micro-environment, mouse melanoma cell line B16F10 (5×10^5 per mouse) in a total volume of 100 μL of buffered saline was subcutaneously injected into the back of C57BL/6 mice, respectively. Tumor size was measured every 2 days with caliper, and tumor volume was calculated on the basis of two-dimensional measurements. Mouse survival was determined on the basis of the tumor sizes calculated according to a standard formula ($\text{length} \times \text{width}^2 \times 0.5$). The experiments were terminated for ethical considerations at the end point (tumor volume, $>1500 \text{ mm}^3$), and mouse survival was then determined. Spleen was harvested, and CD4^+ and CD8^+ T cells were purified for subsequent SA- β -gal staining. In addition, CD4^+ and CD8^+ T cells from indicated organs of normal littermates were harvested and used as negative controls.

4.2 | Cell culture and treatment

Mouse CD8^+ T cells were purified by Miltenyi enrichment kits (Miltenyi Biotec) and activated in the presence of plate-coated anti-mouse CD3 (2 $\mu\text{g}/\text{mL}$), anti-mouse CD28 (1 $\mu\text{g}/\text{mL}$) antibodies. T cells were maintained in T cell medium containing 10% fetal bovine serum, L-glutamine, β -mercaptoethanol, and recombinant human IL-2 (50 U/mL) for 3 days. Melanoma (B16F10) cell lines were purchased from the American Type Culture Collection. Tumor cell lines were cultured in RPMI 1640 containing 10% fetal bovine serum.

4.3 | SA- β -gal staining and quantitative assay

SA- β -gal activity in senescent T cells was detected as previously described. For tumor cell-induced senescent mice, isolated CD8^+ T cells and anti-CD3-activated were cultured for additional 3 days and then stained with SA- β -gal staining reagent (Cell signaling technology, #9860) at $\text{pH} = 6$, according to manufacturer's instructions. Quantitation of SA- β -gal activity was evaluated using Cellular Senescence Plate Assay Kit-SPiDER- β Gal, a fluorogenic substrate for β -galactosidase (Dojindo), following the manufacturer's instructions.

4.4 | NAD⁺ detection

NAD⁺ and NADH were measured with a commercially available NAD⁺/NADH Microplate Assay Kit (Absin,

#abs580008) according to the manufacturer's protocol. For cells, 1×10^6 cells homogenized in 100 μL Assay Buffer I/II and sonicate (with power 20%, sonication 2 s, interval 1 s, repeat 30 times). For mice tissue, 50 mg were homogenized in 100 μL Assay Buffer I/II. Incubate at 60°C for 20 min; centrifuged at 8000g, 4°C for 10 min, take the supernatant into a new centrifuge tube and add 100 μL Assay Buffer II/I, mix; keep it on ice for detection. Standard curves (0.5–50 μM) were generated for quantification.

4.5 | ATP detection

ATP levels were measured with a commercially available ATP Microplate Assay Kit (Absin, abs580117) according to the manufacturer's protocol. Collect cell into centrifuge tube, discard the supernatant after centrifugation, add 1 mL Assay buffer I for 5×10^6 cell, sonicate (with power 20%, sonicate 3 s, interval 10 s, repeat 30 times), centrifuged at 8000g, 4°C for 10 min, take the supernatant into a new centrifuge tube, and keep it on ice for detection. Standard curves (0.02–2.5 mM) were generated for quantification.

4.6 | Flow cytometry analysis

T cell protein expression was determined by flow cytometry analysis after surface staining with anti-mouse specific antibodies, PE anti-mouse CD8a Antibody (BioLegend) and PerCP/Cyanine5.5 anti-mouse CD4 antibody (BioLegend) on ice for 30 min and then washing with phosphate-buffered saline. All stained cells were analyzed on an LSR II cytometer (BD Biosciences), and data were analyzed with FlowJo software (BD Biosciences).

4.7 | Intracellular ROS production assays

For determination of ROS production, CD8^+ T cells were treated with 10 μM 2',7'-Dichlorodihydrofluorescein (DCFH-DA) (Beyotime) at 37°C for 30 min and then washed with PBS 3 times as manufacturer's protocols.

4.8 | Mitochondrial membrane potential detection

Mitochondrial membrane potential measured with JC-1 which is a marker of mitochondrial activity. In normal undamaged nucleate cells, mitochondrion have a high mitochondrial transmembrane potential

($\Delta\Psi_m$). Breakdown of $\Delta\Psi_m$ is characteristic of damage. Cells containing forming J-aggregates have high $\Delta\Psi_m$, and show red fluorescence. Cells with low $\Delta\Psi_m$ are those in which JC-1 maintains (or reacquire) monomeric form, and showing green fluorescence. Depolarization of $\Delta\Psi_m$ was measured by JC-1 which accumulates in mitochondrial matrix, driven by $\Delta\Psi_m$, and expressed as an increase of red to green fluorescent reflecting the transformation of JC-1 aggregates into monomers when mitochondrial membrane becomes depolarized.

4.9 | ELISA

Supernatants were harvested and centrifuged at 1000g to remove cell debris and dead cells. ELISA was performed following the instructions of the Mouse IL1- β (#abs520001), IL-6 (#abs520004), TNF- α (#520010), and IFN- γ (#520007) ELISA Set from Absin.

4.10 | Immunofluorescence staining of STING

Cells were cultured in 35 mm glass-bottomed poly-D-lysine-coated dishes, fixed in 4% buffered formalin with PBS, permeabilized with cold PBS containing 0.1% Triton X-100 for 30 min, and blocked with 4% bovine serum in PBS for 1 h at room temperature. This was followed by incubation with primary anti-STING (Cat No: 19851-1-AP, Proteintech) antibody at 4° for 16 h, and then with CoraLite488-conjugated Goat Anti-Rabbit IgG(H + L) (1:400) antibody at room temperature for 1 h. Cells were costained with DAPI (MBD0015, Sigma-Aldrich) to visualize the nuclei. Immunofluorescence images were then taken under a fluorescence microscope.

4.11 | RNA extraction and quantitative reverse transcription polymerase chain reaction (PCR) analyses

The total RNAs of the CD8⁺ T cells and tissues were extracted with TRIzol reagent (Invitrogen). Reverse-transcribed complementary DNA was performed with random primers. Subsequently, 7500 Real-Time PCR System (AB Applied Biosystems, Mannheim, Germany) was used to run programs of real-time PCR following the manufacturer's instructions. β -actin was used for internal crossing normalization. The primers used for the different genes are listed in Table 1.

4.12 | Quantification of mtDNA in cytosolic extracts

CD8⁺ T cells (approximately 2×10^6) isolated from the spleen of Tumor-free, B16F10-bearing and B16 + NMN mice were divided into 2 equal aliquots. One aliquot was resuspended in roughly 500 μ L of 50 μ M NaOH and boiled for 30 min to solubilize DNA. Approximately 50 μ L of 1 M Tris-HCl (pH 8.0) was added to neutralize the pH of the lysate, and the extracts served as normalization controls for total mtDNA. The second aliquot was resuspended in roughly 500 μ L buffer containing 150 mM NaCl, 50 mM HEPES (pH = 7.4), and 20 μ g/mL digitonin. The homogenates were incubated for 10 min to allow selective plasma permeabilization, and then centrifuged at 980g for 3 min, 3 times to pellet intact cells. The first pellet was saved as the "Pel" fraction for WB analysis. The cytosolic supernatants were transferred into fresh tubes and spun at 17 000g in a microcentrifuge for 10 min to pellet any remaining cellular debris, yielding cytosolic preparations free of nuclear, mitochondrial, and ER contamination. DNA was then purified from these pure cytosolic fractions using the DNA Clean and Concentrator-5 kit (ZYMO Research). qPCR was performed for both whole-cell extracts and cytosolic fractions using nuclear DNA primers (Tert) and mtDNA primers (CytB, 16S, and Dloop1), and the Ct values obtained for mtDNA abundance for whole-cell extracts served as normalization controls for the mtDNA values determined from the cytosolic fractions. The primers used for the different genes are listed in Table 1.

4.13 | West blotting analysis

Western blot analysis was performed according to manufacturer's instructions. Briefly, cell or tissue transformed into cold radio-immunoprecipitation assay lysis buffer containing phenylmethylsulfonyl fluoride (1:100 dilution) (Beyotime Biotechnology) for 30 min. Then, samples were centrifuged at 4°C for 10 min at 12 000 rpm. Supernatants were recovered, and total amounts of protein were determined using the bicinchoninic acid method (Boster Biological Technology). A 50 μ g of protein were loaded on 10% sodium dodecyl sulfate-polyacrylamide gel and transferred onto a polyvinylidene difluoride membrane (Millipore). To avoid nonspecific binding, 5% (wt/vol) dry nonfat milk in tris-buffered saline with Tween 20 (TBST) was used for blocking. After 2 h, the membranes were incubated with primary antibodies to cGAS/STING/p-TBK1/TBK1/p-IRF3/IRF3/P21 (1:1000 dilution, CST), Pink1 (1:2000

TABLE 1 Oligonucleotide primers for qPCR.

Target	Sequence
Mouse- β -actin (F)	CTAAGGCCAACCGTGAAAAG
Mouse- β -actin (R)	ACCAGAGGCATACAGGGACA
Mouse-cGAS (F)	GGAAATAGTTTCAAGGAGAGACC
Mouse-cGAS (R)	TGCATCCAGCTCTTGAAACTC
Mouse-STING (F)	TCCTGGGCCTTCAGAGCTT
Mouse-STING (R)	GTACAGTCTTCGGCTCCCTG
Mouse-TBK1 (F)	TGCCGTTTAGACCCTTCGAG
Mouse-TBK1 (R)	GTGCCTGAAGACCCTGAGAA
Mouse-IRF3 (F)	CAATTCCTCCCTGGCTAGA
Mouse-IRF3 (R)	TTCCACGGGATCCTGAACCT
Mouse-Pink1 (F)	GACCTGAAATCCGACAACATCC
Mouse-Pink1 (R)	CCATCAGACAGCCGTTTCC
Mouse-P21 (F)	CAGCAGAATAAAAGGTGCCACA
Mouse-P21 (R)	GACAACGGCACACTTTGCTC
Mouse-P16 (F)	TGAATCTCCGCGAGGAAAGC
Mouse-P16 (R)	TGCCCATCATCATCACCTGAA
Mouse-Ccl5 (F)	ATATGGCTCGACACCACTC
Mouse-Ccl5 (R)	CTTCGAGTGACAAACACGACTG
Mouse-Isg15 (F)	TCTGACTGTGAGAGCAAGCAG
Mouse-Isg15 (R)	ACCTTTAGGTCCCAGGCCATT
Mouse-Ifit1 (F)	TCTGCTCTGCTGAAAACCCA
Mouse-Ifit1 (R)	CACCATCAGCATTCTCTCCCAT
Mouse-IL1 β (F)	TGCCACCTTTTGACAGTGATG
Mouse- IL1 β (R)	ATGTGCTGCTGCGAGATTTG
Mouse-IL6 (F)	ACAAAGCCAGAGTCCTTCAGAG
Mouse-IL6 (R)	TGTGACTCCAGCTTATCTCTTGG
Mouse-TNF- α (F)	AAGTTCCCAAATGCCTCCC
Mouse-TNF- α (R)	CCACTGGTGGTTTGTGAGTG
Mouse-IFN γ (F)	GGCTGTTTCTGGCTGTTACTG
Mouse-IFN γ (R)	ATTTTCATGTCACCATCCTTTTGCC
Mouse-nucDNA Tert (F)	CTAGCTCATGTGTCAAGACCCTCTT
Mouse-nucDNA Tert (R)	GCCAGCACGTTTCTCTCGTT
Mouse-mtDNA CytB (F)	GCTTCCACTTCATCTTACCATTTA
Mouse-mtDNA CytB (R)	TGTTGGGTTGTTTGATCCTG
Mouse-mtDNA 16 S (F)	CACTGCCTGCCAGTGA

TABLE 1 (Continued)

Target	Sequence
Mouse-mtDNA 16 S (R)	ATACCGCGGCCGTTAAA
Mouse-mtDNA Dloop1 (F)	AATCTACCATCCTCCGTGAAACC
Mouse-mtDNA Dloop1 (R)	TCAGTTTAGCTACCCCAAGTTTAA

dilution, Absin), β -actin (1:4000 dilution, Absin) overnight at 4°C. After washing the membranes with TBST for three times, membranes were incubated with goat anti-rabbit or goat anti-mouse secondary antibodies conjugated to immunoglobulin G- horseradish peroxidase (1:10000 dilution). Followed by additional washing with TBST, the proteins were visualized using enhanced chemiluminescence. Bands were quantified with Image J (National Institutes of Health).

4.14 | Statistical analysis

Quantitative data are presented as the mean \pm SD. Analysis of the variance (ANOVA) with Tukey post hoc test (one-way ANOVA for comparisons between groups) was applied to compare values among different experimental groups using GraphPad Prism (GraphPad Software). Statistical differences of two groups were assessed using unpaired Student's *t* test, *t*-test with Welch's correction for variance where appropriate. **p* < 0.05 was considered statistically significant, ***p* < 0.01 was considered highly significant, ****p* < 0.001 and *****p* < 0.0001 were considered extremely significant. The Kaplan-Meier estimator and log-rank (Mantel-Cox) test was used for survival analysis of tumor-bearing mice.

AUTHOR CONTRIBUTIONS

Bin Ye, Lujing Wan, Yu Qiao, Xu Gao, Yanfen Zhang, and Ning Ma designed experiments. Bin Ye, Yingting Pei, Yu Zhang, Dehao Meng, Shuang Zou, and Henian Li performed animal treatment and behavior test. Bin Ye, Yingting Pei, Ziyang Xie, and Jinying Liu collected the tissues from animals. Bin Ye, Yingting Pei, Changhong Tian, Yuqi Jiang, and Yu Zhang performed Western blot analysis, IF, ELISA, qPCR, mitochondrial analysis, and cellular experiments. Bin Ye, and Yingting Pei performed tissue preparation. Bin Ye and Yingting Pei performed microarray analysis. Bin Ye wrote and Bin Ye, Lujing Wang, Xu Gao, Yu Qiao, Yanfen Zhang, and

Ning Ma revised the manuscript. All authors contributed to writing the final manuscript.

ACKNOWLEDGMENTS

This study was supported by the Key projects of National Key Research and Development Program “Inter-governmental Cooperation in Science and Technology Innovation” (2022YFE0118200), Natural Science Foundation of Heilongjiang Province (ZD2022H004), Reserve leader project of Heilongjiang Provincial leading talent Echelon (2018), Young Marshal Unveiling Project of Harbin Medical University (HMUMIF-21025), and Young & middle-aged Innovative Scientific Research Fund of the Second Affiliated Hospital of Harbin Medical University (KYCX2019-14).

CONFLICT OF INTEREST STATEMENT

The authors declare no conflict of interest.

DATA AVAILABILITY STATEMENT

The data that supports the findings of this study are available from the corresponding author.

ORCID

Bin Ye  <http://orcid.org/0009-0001-2987-0769>

REFERENCES

- Campisi J. Aging, cellular senescence, and cancer. *Annu Rev Physiol.* 2013;75:685-705. doi:10.1146/annurev-physiol-030212-183653
- Signer RAJ, Morrison SJ. Mechanisms that regulate stem cell aging and life span. *Cell Stem Cell.* 2013;12:152-165. doi:10.1016/j.stem.2013.01.001
- Bonafè M, Sabbatinelli J, Olivieri F. Exploiting the telomere machinery to put the brakes on inflamm-aging. *Ageing Res Rev.* 2020;59:101027. doi:10.1016/j.arr.2020.101027
- Ferrucci L, Fabbri E. Inflammageing: chronic inflammation in ageing, cardiovascular disease, and frailty. *Nat Rev Cardiol.* 2018;15:505-522. doi:10.1038/s41569-018-0064-2
- Salminen A, Kaarniranta K, Kauppinen A. Immunosenescence: the potential role of myeloid-derived suppressor cells (MDSC) in age-related immune deficiency. *Cell Mol Life Sci.* 2019;76:1901-1918. doi:10.1007/s00018-019-03048-x
- Krichevsky S, Pawelec G, Gural A, et al. Age related microsatellite instability in T cells from healthy individuals. *Exp Gerontol.* 2004;39:507-515. doi:10.1016/j.exger.2003.12.016
- Tarasenko TN, Pacheco SE, Koenig MK, et al. Cytochrome c oxidase activity is a metabolic checkpoint that regulates cell fate decisions during T cell activation and differentiation. *Cell Metab.* 2017;25(1254-1268):1254-1268. doi:10.1016/j.cmet.2017.05.007
- Effros RB. Replicative senescence in the immune system: impact of the hayflick limit on T-cell function in the elderly. *The Am J Human Genet.* 1998;62:1003-1007. doi:10.1086/301845
- Bouso P. T-cell activation by dendritic cells in the lymph node: lessons from the movies. *Nat Rev Immunol.* 2008;8:675-684. doi:10.1038/nri2379
- Dolfi DV, Katsikis PD. CD28 and CD27 costimulation of CD8+ T cells: a story of survival. *Adv Exp Med Biol.* 2007;590:149-170. doi:10.1007/978-0-387-34814-8_11
- Onyema OO, Njemini R, Forti LN, et al. Aging-associated subpopulations of human CD8+ t-lymphocytes identified by their CD28 and CD57 phenotypes. *Arch Gerontol Geriat.* 2015;61:494-502. doi:10.1016/j.archger.2015.08.007
- Rongvaux A, Jackson R, Harman CCD, et al. Apoptotic caspases prevent the induction of type I interferons by mitochondrial DNA. *Cell.* 2014;159:1563-1577. doi:10.1016/j.cell.2014.11.037
- West AP, Khoury-Hanold W, Staron M, et al. Mitochondrial DNA stress primes the antiviral innate immune response. *Nature.* 2015;520:553-557. doi:10.1038/nature14156
- White MJ, McArthur K, Metcalf D, et al. Apoptotic caspases suppress mtDNA-induced STING-mediated type I IFN production. *Cell.* 2014;159:1549-1562. doi:10.1016/j.cell.2014.11.036
- Desdín-Micó G, Soto-Herederó G, Aranda JF, et al. T cells with dysfunctional mitochondria induce multimorbidity and premature senescence. *Science.* 2020;368:1371-1376. doi:10.1126/science.aax0860
- Dou Z, Ghosh K, Vizioli MG, et al. Cytoplasmic chromatin triggers inflammation in senescence and cancer. *Nature.* 2017;550:402-406. doi:10.1038/nature24050
- Moretti J, Roy S, Bozec D, et al. STING senses microbial viability to orchestrate stress-mediated autophagy of the endoplasmic reticulum. *Cell.* 2017;171(809-823):809-823. doi:10.1016/j.cell.2017.09.034
- Motwani M, Pesiridis S, Fitzgerald KA. DNA sensing by the cGAS-STING pathway in health and disease. *Nat Rev Genet.* 2019;20:657-674. doi:10.1038/s41576-019-0151-1
- Ablasser A, Chen ZJ. cGAS in action: expanding roles in immunity and inflammation. *Science.* 2019;363(6431):eaat8657. doi:10.1126/science.aat8657
- Chen Q, Sun L, Chen ZJ. Regulation and function of the cGAS-STING pathway of cytosolic DNA sensing. *Nature Immunol.* 2016;17:1142-1149. doi:10.1038/ni.3558
- Li T, Chen ZJ. The cGAS-cGAMP-STING pathway connects DNA damage to inflammation, senescence, and cancer. *J Exp Med.* 2018;215:1287-1299. doi:10.1084/jem.20180139
- Yang H, Wang H, Ren J, Chen Q, Chen ZJ. cGAS is essential for cellular senescence. *Proc Natl Acad Sci.* 2017;114:E4612-e4620. doi:10.1073/pnas.1705499114
- Hertz NT, Berthet A, Sos ML, et al. A neo-substrate that amplifies catalytic activity of parkinson's-disease-related kinase PINK1. *Cell.* 2013;154:737-747. doi:10.1016/j.cell.2013.07.030
- Sliter DA, Martinez J, Hao L, et al. Parkin and PINK1 mitigate STING-induced inflammation. *Nature.* 2018;561:258-262. doi:10.1038/s41586-018-0448-9
- Lin MT, Beal MF. Mitochondrial dysfunction and oxidative stress in neurodegenerative diseases. *Nature.* 2006;443:787-795. doi:10.1038/nature05292
- Lan YY, Heather JM, Eisenhaure T, et al. Extranuclear DNA accumulates in aged cells and contributes to senescence and inflammation. *Ageing cell.* 2019;18:e12901. doi:10.1111/acer.12901
- Fang EF, Lautrup S, Hou Y, et al. NAD(+) in aging: molecular mechanisms and translational implications. *Trends Mol Med.* 2017;23:899-916. doi:10.1016/j.molmed.2017.08.001

28. Covarrubias AJ, Perrone R, Grozio A, Verdin E. NAD(+) metabolism and its roles in cellular processes during ageing. *Nat Rev Mol Cell Biol.* 2021;22:119-141. doi:10.1038/s41580-020-00313-x
29. Surjana D, Halliday GM, Damian DL. Role of nicotinamide in DNA damage, mutagenesis, and DNA repair. *J Nucleic Acids.* 2010;2010:157591. doi:10.4061/2010/157591
30. Hou Y, Lautrup S, Cordonnier S, et al. NAD(+) supplementation normalizes key alzheimer's features and DNA damage responses in a new AD mouse model with introduced DNA repair deficiency. *Proceedings of the National Academy of Sciences.* 2018;115:E1876-e1885. doi:10.1073/pnas.1718819115
31. Wang Y, Li Y, He C, Gou B, Song M. Mitochondrial regulation of cardiac aging. *Biochim Biophys Acta, Mol Basis Dis.* 2019;1865:1853-1864. doi:10.1016/j.bbadis.2018.12.008
32. Mills KF, Yoshida S, Stein LR, et al. Long-Term administration of nicotinamide mononucleotide mitigates Age-Associated physiological decline in mice. *Cell Metab.* 2016;24:795-806. doi:10.1016/j.cmet.2016.09.013
33. Ryu D, et al. NAD+ repletion improves muscle function in muscular dystrophy and counters global PARylation. *Sci Transl Med.* 2016;8:361ra139. doi:10.1126/scitranslmed.aaf5504
34. Thommen DS, Schumacher TN. T cell dysfunction in cancer. *Cancer Cell.* 2018;33:547-562. doi:10.1016/j.ccell.2018.03.012
35. Liu X, Hartman CL, Li L, et al. Reprogramming lipid metabolism prevents effector T cell senescence and enhances tumor immunotherapy. *Sci Transl Med.* 2021;13(587):eaa6314. doi:10.1126/scitranslmed.aaz6314
36. Ye J, Ma C, Hsueh EC, et al. Tumor-derived $\gamma\delta$ regulatory T cells suppress innate and adaptive immunity through the induction of immunosenescence. *J Immunol.* 2013;190:2403-2414. doi:10.4049/jimmunol.1202369
37. McArthur K, Whitehead LW, Heddleston JM, et al. BAK/BAX macropores facilitate mitochondrial herniation and mtDNA efflux during apoptosis. *Science.* 2018;359(6378):eaa6047. doi:10.1126/science.aao6047
38. Song X, Ma F, Herrup K. Accumulation of cytoplasmic DNA due to ATM deficiency activates the microglial viral response system with neurotoxic consequences. *J Neurosci.* 2019;39:6378-6394. doi:10.1523/jneurosci.0774-19.2019
39. Aarreberg LD, Esser-Nobis K, Driscoll C, Shuvarikov A, Roby JA, Gale Jr. M. Interleukin-1 β induces mtDNA release to activate innate immune signaling via cGAS-STING. *Mol Cell.* 2019;74(801-815):801-815. doi:10.1016/j.molcel.2019.02.038
40. Durcan TM, Fon EA. The three 'p's of mitophagy: PARKIN, PINK1, and post-translational modifications. *Genes Dev.* 2015;29:989-999. doi:10.1101/gad.262758.115
41. Matsuda S, Kitagishi Y, Kobayashi M. Function and characteristics of PINK1 in mitochondria. *Oxid Med Cell Longevity.* 2013;2013:601587. doi:10.1155/2013/601587
42. Fang EF, Hou Y, Palikaras K, et al. Mitophagy inhibits amyloid- β and tau pathology and reverses cognitive deficits in models of alzheimer's disease. *Nature Neurosci.* 2019;22:401-412. doi:10.1038/s41593-018-0332-9
43. Baker DJ, Petersen RC. Cellular senescence in brain aging and neurodegenerative diseases: evidence and perspectives. *J Clin Invest.* 2018;128:1208-1216. doi:10.1172/jci95145
44. López-Otín C, Blasco MA, Partridge L, Serrano M, Kroemer G. The hallmarks of aging. *Cell.* 2013;153:1194-1217. doi:10.1016/j.cell.2013.05.039
45. Acosta JC, O'Loughlin A, Banito A, et al. Chemokine signaling via the CXCR2 receptor reinforces senescence. *Cell.* 2008;133:1006-1018. doi:10.1016/j.cell.2008.03.038
46. Kuilman T, Michaloglou C, Vredeveld LCW, et al. Oncogene-induced senescence relayed by an interleukin-dependent inflammatory network. *Cell.* 2008;133:1019-1031. doi:10.1016/j.cell.2008.03.039
47. Mills EL, Kelly B, O'Neill LAJ. Mitochondria are the powerhouses of immunity. *Nature Immunol.* 2017;18:488-498. doi:10.1038/ni.3704
48. Sena LA, Li S, Jairaman A, et al. Mitochondria are required for antigen-specific T cell activation through reactive oxygen species signaling. *Immunity.* 2013;38:225-236. doi:10.1016/j.immuni.2012.10.020
49. Verdin E. NAD+ in aging, metabolism, and neurodegeneration. *Science.* 2015;350:1208-1213. doi:10.1126/science.aac4854
50. Zhang H, Ryu D, Wu Y, et al. NAD+ repletion improves mitochondrial and stem cell function and enhances life span in mice. *Science.* 2016;352:1436-1443. doi:10.1126/science.aaf2693
51. Katsyuba E, Mottis A, Zietak M, et al. De novo NAD+ synthesis enhances mitochondrial function and improves health. *Nature.* 2018;563:354-359. doi:10.1038/s41586-018-0645-6
52. Elhassan YS, Kluckova K, Fletcher RS, et al. Nicotinamide riboside augments the aged human skeletal muscle NAD+ metabolome and induces transcriptomic and anti-inflammatory signatures. *Cell Rep.* 2019;28:1717-1728.e6. doi:10.1016/j.celrep.2019.07.043
53. Hou Y, Wei Y, Lautrup S, et al. NAD+ supplementation reduces neuroinflammation and cell senescence in a transgenic mouse model of Alzheimer's disease via cGAS-STING. *Proc Natl Acad Sci.* 2021;118(37):e2011226118. doi:10.1073/pnas.2011226118
54. Fang EF, Kassahun H, Croteau DL, et al. NAD+ replenishment improves lifespan and healthspan in ataxia telangiectasia models via mitophagy and DNA repair. *Cell Metab.* 2016;24:566-581. doi:10.1016/j.cmet.2016.09.004

How to cite this article: Ye B, Pei Y, Wang L, et al. NAD⁺ supplementation prevents STING-induced senescence in CD8⁺ T cells by improving mitochondrial homeostasis. *J Cell Biochem.* 2024; 1-17. doi:10.1002/jcb.30522